Eur. Phys. J. C (2019) 79:155
https://doi.org/10.1140/epjc/s10052-019-6661-3

THE EUROPEAN PHYSICAL JOURNAL C

Regular Article - Theoretical Physics

Freeze-out conditions from strangeness observables at RHIC

Marcus Bluhm[1,a], **Marlene Nahrgang**[2,b]

[1] Institute of Theoretical Physics, University of Wrocław, 50-204 Wrocław, Poland
[2] SUBATECH UMR 6457 (IMT Atlantique, Université de Nantes, IN2P3/CNRS), 4 rue Alfred Kastler, 44307 Nantes, France

Received: 2 July 2018 / Accepted: 8 February 2019 / Published online: 20 February 2019

Abstract We determine chemical freeze-out conditions from strangeness observables measured at RHIC beam energies. Based on a combined analysis of lowest-order net-kaon fluctuations and strange anti-baryon over baryon yield ratios we obtain visibly enhanced freeze-out conditions at high beam energies compared to previous studies which analyzed net-proton and net-charge fluctuations. Our findings are in qualitative agreement with the recent study (Bellwied et al. in arXiv:1805.00088 [hep-ph], 2018) which utilizes the net-kaon fluctuation data in combination with information from lattice QCD. Our complementary approach shows that also strange hadron yield ratios are described by such enhanced freeze-out conditions.

1 Introduction

High-energy heavy-ion collision experiments at various beam energies $\sqrt{s_{NN}}$ have enriched our understanding of the properties and phases of strongly interacting matter. The transient creation of a color-deconfined state in the laboratories was one of the major scientific successes in the last two decades. The deconfinement transition is an analytic crossover for vanishing baryon chemical potential μ_B [2], where the transition region $T_c = (154 \pm 9)$ MeV [3,4] is rather broad in temperature T. While these information base on first-principle lattice QCD calculations, another fascinating landmark in the phase diagram, the QCD critical point, has not yet been discovered with this method despite being predicted by various approaches [5,6].

Information about the properties of hot and dense QCD matter can be inferred indirectly from the measured particle spectra and their event-by-event fluctuations. The success of statistical hadronization models in describing the particle production in heavy-ion collisions ranging from AGS to LHC beam energies [7–10] led to the conclusion that the produced hadronic matter originates from a source in or near thermal and chemical equilibrium. A common freeze-out curve [7] in the phase diagram could be drawn, highlighting the thermal conditions (T, μ_B) at chemical freeze-out where the hadrochemistry is fixed.

Higher-order moments of the event-by-event particle multiplicity distributions provide an additional excellent measure to characterize the matter properties and to reveal the phase structure in QCD. While it is debated whether fluctuations originate from an equilibrated hadronic medium [11,12] it is to a first extent reasonable to assume, that if this is true for the means also the lowest-order fluctuations, i.e. the variances, should be describable within statistical models. First studies [13,14], utilizing experimental data on net-proton and net-electric charge fluctuations to determine the freeze-out conditions, found at large $\sqrt{s_{NN}}$ significantly reduced freeze-out parameters compared to [7]. In the work [13], the analysis was quantitatively driven by the contributions from protons and anti-protons as well as charged pions.

In a recent study [1], the experimental data [15] on lowest-order fluctuations in the net-kaon number $N_{K^+} - N_{K^-}$ as function of $\sqrt{s_{NN}}$ were used to extract freeze-out conditions. For a unique determination, information from lattice QCD for the isentropic trajectories [16] running through the freeze-out points of [13] was supplemented. The obtained freeze-out temperatures were reported to be substantially larger than those found in [13]. In our work, we combine an analysis of the net-kaon fluctuations [15] and the yield ratios of strange anti-baryons over baryons [17–19] as functions of $\sqrt{s_{NN}}$. This complementary approach allows us to determine whether strange baryon yields and net-kaon fluctuations can be described with the same T and μ_B.

Our strategy is to analyze observables that are highly sensitive to variations in the thermal parameters. As we discussed in [20], the ratio of variance over mean of the net-kaon number is such an observable that varies rapidly with T in a statistical model. The same is true for the heavier baryons

[a] e-mail: marcus.bluhm@ift.uni.wroc.pl
[b] e-mail: marlene.nahrgang@subatech.in2p3.fr

while we use the lighter baryons as a baryometer in this work. Therefore, we consider the combination of observables studied here as optimized for determining freeze-out conditions. One should keep in mind, nevertheless, that the net-kaon number is not a conserved charge in QCD and as such prone to late stage processes like resonance decays.

2 Theoretical framework

We perform our analysis of net-kaon fluctuations and strange anti-baryon to baryon yield ratios using a Hadron Resonance Gas (HRG) model for a grandcanonical ensemble of non-interacting hadrons and resonances. Such a model, in which the strong interaction between hadrons is effectively accounted for by contributions from resonances [21], was shown to reliably describe basic thermodynamic quantities [22–24] as well as susceptibilities and their ratios [25–27] from lattice QCD. The hadrons and resonances are considered to be point-like in our work. The pressure P in this framework reads

$$P = \sum_i (-1)^{B_i+1} \frac{d_i T}{(2\pi)^3} \int \mathrm{d}^3k \ln\left[1 + (-1)^{B_i+1} z_i e^{-\epsilon_i/T}\right], \tag{1}$$

where the sum runs over all particle species included in the framework. In Eq. (1) the particle energy reads $\epsilon_i = \sqrt{k^2 + m_i^2}$ for momentum k and particle mass m_i, d_i is the degeneracy factor and $z_i = e^{\mu_i/T}$ is the fugacity. The particle chemical potential μ_i is defined as $\mu_i = B_i\mu_B + S_i\mu_S + Q_i\mu_Q$, where μ_X denotes the chemical potential of the conserved charge X and $X_i = B_i, S_i, Q_i$ represent the quantum numbers of the conserved baryon, strangeness and electric charge, respectively.

In Eq. (1), we use an updated version of the spectrum of hadrons and resonances in line with the recent listing from the Particle Data Group [28]. In previous studies [29,30], the advantages of using such an update were discussed in detail. Moreover, in [31] the influence of unconfirmed resonances in the 2016 listing [28] versus only confirmed resonances on determined freeze-out parameters was investigated.

The net-density n_X of a conserved charge is given by $n_X = \sum_i X_i n_i$, where the individual particle densities n_i follow from derivatives, $n_i = (\partial P/\partial\mu_i)$, at fixed T. With this, physical conditions met in a heavy-ion collision experiment can be implemented into the model [32] by requiring that $n_S = 0$ and $n_Q = x n_B$. These account for net-strangeness neutrality in the fireball and an initial proton to baryon ratio at mid-rapidity which for Au+Au and Pb+Pb collisions is approximately $x \simeq 0.4$. As a consequence, the chemical potentials μ_S and μ_Q become functions of T and μ_B. Due to the lack of stopping at high $\sqrt{s_{NN}}$, the mid-rapidity region is almost isospin symmetric. As μ_B, and thus n_B, is small for high beam energies this is also approximately satisfied by the second physical condition.

The experimentally realized phase-space coverage, which can be limited in rapidity y, transverse momentum k_T and azimuthal angle ϕ due to the detector design and demands from the analysis, can be respected in a straightforward way. Following [33], kinematic acceptance cuts are implemented into the model by restricting the momentum integrals in Eq. (1) accordingly. This requires replacing the integration measure d^3k by $k_T\sqrt{k_T^2 + m_i^2}\cosh(y)\,\mathrm{d}k_T\,\mathrm{d}y\,\mathrm{d}\phi$ and ϵ_i by $\cosh(y)\sqrt{k_T^2 + m_i^2}$. It should be noted that this procedure does not take into account the elastic scatterings between chemical and kinetic freeze-out, which can transport individual particles in and out of the experimental acceptance. In order to take this correctly into account, a fully dynamical transport approach for the hadronic phase would need to be applied. We think, however, that only a small number of all considered particles are actually affected by this kind of final state effect.

The effect of resonance decays can be implemented into the framework in an explicit way which allows us to keep correctly track of the strangeness transfer from mother to daughter including resonances such as e.g. $\Xi(1690)^-$ or $N(1650)$. This is different from the way resonance decays were implemented in [1]. Our method was developed in [34,35] and applied to study the impact of resonance decays on net-proton fluctuations without [36] and in the presence of a QCD critical point [37]. The final particle number N_j of a stable, i.e. with respect to strong and electromagnetic decays, hadron is given by the sum $N_j = N_j^* + \sum_R \langle N_j^R\rangle_R$ of primordially, i.e. directly, produced hadrons N_j^* and the contributions stemming from resonance decays. Those produce on average over the decays $\langle N_j^R\rangle_R = N_R^*\langle n_j\rangle_R$ hadrons of type j associated with the branching ratios b_r^R of resonance R via $\langle n_j\rangle_R = \sum_r b_r^R n_{j,r}^R$ for integer $n_{j,r}^R$. On an event-by-event basis, the numbers N_j^* and N_R^* fluctuate thermally. But, in addition, the actual number of hadrons of type j originating from the decay of R follows a multinomial probability distribution [34]. Thus, fluctuations in the contributions from resonance decays are caused both by thermal fluctuations in N_R^* and by the probabilistic character of the decay process. For the mean, the latter has no consequences and thus the mean of the final particle number after resonance decays is given by

$$M_j = \langle N_j^*\rangle_T + \sum_R \langle N_R^*\rangle_T \langle n_j\rangle_R\,. \tag{2}$$

Accordingly, for the net-kaon number, the mean is given by $M_K = M_{K^+} - M_{K^-}$. The variance of the net-kaon number

is instead influenced by the probabilistic nature of the decay and follows as [34,35]

$$\begin{aligned}\sigma_K^2 &= \langle(\Delta N_{K^+}^*)^2\rangle_T + \langle(\Delta N_{K^-}^*)^2\rangle_T \\ &+ \sum_R \langle(\Delta N_R^*)^2\rangle_T \left(\langle n_{K^+}\rangle_R^2 + \langle n_{K^-}\rangle_R^2\right) \\ &- 2\sum_R \langle(\Delta N_R^*)^2\rangle_T \langle n_{K^+}\rangle_R \langle n_{K^-}\rangle_R \\ &+ \sum_R \langle N_R^*\rangle_T \left(\langle(\Delta n_{K^+})^2\rangle_R + \langle(\Delta n_{K^-})^2\rangle_R\right) \\ &- 2\sum_R \langle N_R^*\rangle_T \langle \Delta n_{K^+} \Delta n_{K^-}\rangle_R \,, \end{aligned} \tag{3}$$

where $\Delta N_i = N_i - \langle N_i\rangle_T$ and $\langle \Delta n_i \Delta n_l\rangle_R = \langle n_i n_l\rangle_R - \langle n_i\rangle_R \langle n_l\rangle_R = \sum_r b_r^R n_{i,r}^R n_{l,r}^R - \langle n_i\rangle_R \langle n_l\rangle_R$. As apparent from Eq. (3), resonance decays introduce correlations between the number of K^+ and K^-. Neglecting the probabilistic nature of the decay processes, the variance reads instead

$$\begin{aligned}\sigma_K^2 &= \langle(\Delta N_{K^+}^*)^2\rangle_T + \langle(\Delta N_{K^-}^*)^2\rangle_T \\ &+ \sum_R \langle(\Delta N_R^*)^2\rangle_T \left(\langle n_{K^+}\rangle_R^2 + \langle n_{K^-}\rangle_R^2\right) \\ &- 2\sum_R \langle(\Delta N_R^*)^2\rangle_T \langle n_{K^+}\rangle_R \langle n_{K^-}\rangle_R \,. \end{aligned} \tag{4}$$

In Eqs. (2)–(4) only the thermal averages $\langle\cdot\rangle_T$ can be obtained from the HRG model pressure in Eq. (1) as the derivatives

$$\langle N_i\rangle_T = VT^3 \frac{\partial(P/T^4)}{\partial(\mu_i/T)} \equiv V n_i \,, \tag{5}$$

$$\langle(\Delta N_i)^2\rangle_T = VT^3 \frac{\partial^2(P/T^4)}{\partial(\mu_i/T)^2} \,, \tag{6}$$

where V is the volume which cancels in ratios.

3 Analysis and results

We determine the conditions for T and μ_X at chemical freeze-out by applying the framework outlined above to optimally describe experimental data from RHIC on strangeness observables measured by the STAR Collaboration. We analyze data on yield ratios of strange anti-baryons over baryons, $\bar{B}/B$, as well as lowest-order net-kaon fluctuations, σ_K^2/M_K, simultaneously.

For the $\bar{B}/B$-ratios we study the published results in [17,18] for $\sqrt{s_{NN}} = 200$ and 62.4 GeV, and for smaller $\sqrt{s_{NN}}$ the preliminary results from the RHIC Beam Energy Scan reported in [19]. The ratios for most central collisions, shown as functions of $\sqrt{s_{NN}}$ in Fig. 1 (upper panel) for Λ (squares), Ξ^- (triangles) and Ω^- (circles), were determined from ϕ- and k_T-integrated yields in a given rapidity window around mid-rapidity. In line with the experimental set-up, we consider the y-ranges summarized in Table 1.

For the net-kaon fluctuations we take the results recently reported in [15] which are corrected for finite detector efficiency and the centrality bin width effect. The data for most central collisions are shown by the squares in Fig. 1 (lower panel) where we include only the dominating systematic error bars in the plot. For σ_K^2/M_K, the experimental kinematic acceptance limitations are 0.2 GeV/c $\leq k_T \leq$ 1.6 GeV/c and $-0.5 \leq y \leq 0.5$ with full azimuthal coverage.

In the analysis of the data, the contributions from resonance decays play an important role. For example, for the net-kaon fluctuations, significant correlations between K^+ and K^- are induced by the decay processes. For the ratio $\bar{\Lambda}/\Lambda$ we include in addition to the final particle numbers of Λ and $\bar{\Lambda}$ also the contributions from electromagnetic Σ^0 and $\bar{\Sigma}^0$ decays. Those contributions were not corrected in the experimental analysis [17–19].

The optimal fits for $\bar{B}/B$, where the means are obtained via Eq. (2), and σ_K^2/M_K including the reported error bars are shown by the colored bands in Fig. 1. The corresponding freeze-out conditions for T and μ_B are shown in Fig. 2 by the red, solid squares. For comparison, we contrast the freeze-out conditions [13] deduced from an analysis of lowest-order net-proton and net-electric charge fluctuations which are shown by the blue, open squares. Similar to [1], we observe in particular for large $\sqrt{s_{NN}}$ a significant enhancement of the chemical freeze-out temperature compared to [13] while for smaller $\sqrt{s_{NN}}$ the two different results approach each other. Moreover, as in [38], which bases its analysis entirely on hadronic yields distinguishing strange from non-strange hadrons, we find a non-negligible modification of μ_B compared to [13]. Our results and the ones reported in [1] overlap within errors, but our results are systematically smaller in T and larger in μ_B compared to [1]. The determination of the freeze-out temperature is sensitively influenced by the net-kaon fluctuation

Table 1 Summary of considered rapidity windows in the analysis of $\bar{B}/B$-ratios. The beam energy $\sqrt{s_{NN}}$ is given in GeV

$\sqrt{s_{NN}}$	200	62.4	39	27	19.6	11.5
Λ	$\lvert y\rvert < 1$	$\lvert y\rvert < 1$	$\lvert y\rvert < 0.5$	$\lvert y\rvert < 0.5$	$\lvert y\rvert < 0.5$	$\lvert y\rvert < 0.5$
Ξ	$\lvert y\rvert < 0.75$	$\lvert y\rvert < 1$	$\lvert y\rvert < 0.5$	$\lvert y\rvert < 0.5$	$\lvert y\rvert < 0.5$	$\lvert y\rvert < 0.5$
Ω	$\lvert y\rvert < 1$	$\lvert y\rvert < 1$	$\lvert y\rvert < 0.5$	$\lvert y\rvert < 0.5$	$\lvert y\rvert < 0.5$	$\lvert y\rvert < 0.5$

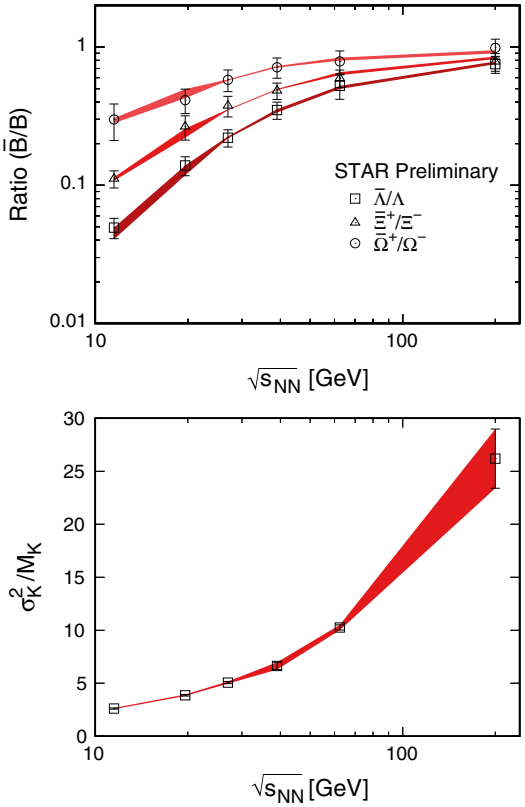

Fig. 1 Upper panel: Ratio $\bar{B}/B$ of strange anti-baryon over baryon yields for Λ, Ξ^- and Ω^- as a function of the beam energy $\sqrt{s_{NN}}$. The published and preliminary STAR data (symbols) are taken from [17–19], respectively. The colored bands show the fit results for $\bar{B}/B$ within the employed HRG model for the freeze-out conditions determined in this work. Lower panel: Lowest-order net-kaon fluctuation measure σ_K^2/M_K of variance σ_K^2 over mean M_K as function of $\sqrt{s_{NN}}$. The published STAR data (squares) are taken from [15], where the shown error bars indicate only the dominating systematic error. The colored band depicts our fit results for the freeze-out conditions shown in Fig. 2

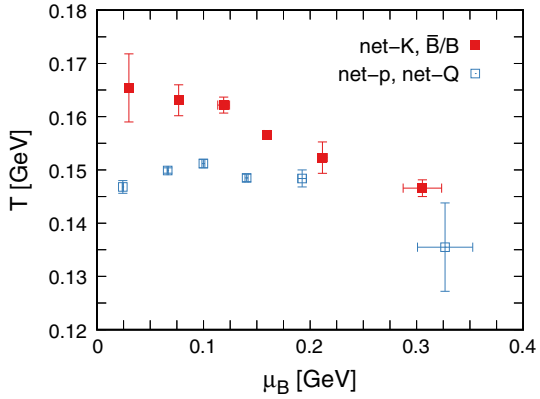

Fig. 2 Chemical freeze-out conditions for T and μ_B determined for the beam energies $\sqrt{s_{NN}} = 200, 62.4, 39, 27, 19.6, 11.5$ GeV (from left to right). The red, solid squares show the results determined in this work from the combined analysis of lowest-order net-kaon fluctuations, σ_K^2/M_K, and $\bar{B}/B$ yield ratios. The error bars correspond to the bands in the fits shown in Fig. 1. The blue, open squares depict the freeze-out conditions reported in [13] which were determined from a combined analysis of lowest-order net-proton and net-electric charge fluctuations

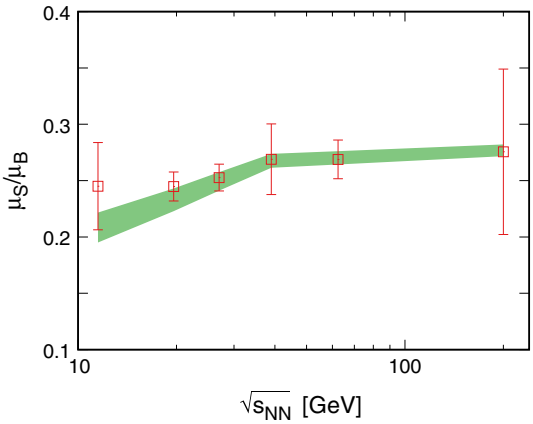

Fig. 3 Ratio μ_S/μ_B of strangeness over baryon chemical potential as a function of $\sqrt{s_{NN}}$ (red, open squares) for the freeze-out conditions shown in Fig. 2. The error bars account for the bands in the fits shown in Fig. 1. Using our determined central values for T and μ_B we show, in comparison, the corresponding lattice QCD ratio $\mu_S/\mu_B = s_1(T) + s_3(T)\mu_B^2$ (colored band), where the bandwidth is deduced from the data on $s_1(T)$ and $s_3(T)/s_1(T)$ and their errors reported in [25]

data as was already discussed in [20]. Here, our use of the heavier (anti-)baryons adds sensitivity to T, while the lighter (anti-)baryons influence stronger the determination of μ_B.

The electric charge chemical potential μ_Q is negative and negligibly small compared to μ_B. In contrast, the strangeness chemical potential μ_S constitutes a non-negligible fraction of μ_B according to the condition of strangeness neutrality as was stressed in previous lattice QCD studies [25,39]. In Fig. 3, we depict our results for the ratio μ_S/μ_B (red, open squares) for the freeze-out conditions shown in Fig. 2. The relatively large errors in μ_S/μ_B are a consequence of the errors in μ_B and in T and the imposed strangeness neutrality. For comparison, we also show the lattice QCD result $\mu_S/\mu_B = s_1(T) + s_3(T)\mu_B^2$ (colored band) evaluated for the central values of T and μ_B determined in this work using the data on $s_1(T)$ and $s_3(T)/s_1(T)$ published in [25]. The bandwidth results from the error bars reported there.

Finally, the importance of the fluctuation contributions due to the probabilistic character of resonance decays can be tested explicitly in our framework. Leaving these contributions out, the variance σ_K^2 is given by Eq. (4), while the mean remains unaffected. Performing the analysis of the experimental data again with this set-up, we find a reduction of the determined freeze-out temperature by about 5%, while the obtained μ_B is up to 18% underestimated. This highlights that, indeed, the probabilistic nature of the decay processes influences our final results in a non-negligible way.

4 Conclusions and outlook

In this work we determined chemical freeze-out conditions by analyzing strangeness observables from RHIC measurements at different beam energies. In our analysis we studied both the lowest-order net-kaon fluctuations in [15] and strange anti-baryon over baryon yield ratios from [17–19] within a Hadron Resonance Gas model framework. From the combined optimized fit, the freeze-out temperature as well as the chemical potentials associated with the conserved charges of QCD were inferred. We find that the obtained freeze-out temperature is significantly enhanced at large $\sqrt{s_{NN}}$ compared to the results of a previous study [13] which used data on net-proton and net-electric charge fluctuations instead. The baryon chemical potential is also visibly enhanced compared to [13] except for the smallest $\sqrt{s_{NN}}$. For smaller $\sqrt{s_{NN}}$, the freeze-out conditions from both approaches start to converge. We note that the results for T and μ_B determined in this work are compatible within errors with those from the statistical hadronization model fits of hadron yields (or ratios) [7–10].

The results presented here are in qualitative agreement with the findings of a recent study [1] which used the net-kaon fluctuation data supplemented by information from lattice QCD. Our complementary study shows that also measured yield ratios of strange anti-baryons over baryons can be described by similar freeze-out conditions. For a precise determination of the latter, the correct implementation of resonance decay contributions plays an important role. We find that resonance decays lead, for example, to significant correlations between K^+ and K^- reducing the lowest-order fluctuation measure σ_K^2/M_K of the net-kaon number by about 15% from its Skellam limit for the same thermal parameters.

The freeze-out conditions presented in Figs. 2 and 3 are, of course, subject to both the quality of the analyzed data and limitations in the applied framework. The data on $\bar{B}/B$-ratios from the Beam Energy Scan [19] are still preliminary and therefore quantitative changes in the determined freeze-out conditions at these $\sqrt{s_{NN}}$ can be expected for future published data, especially in terms of the considered error bars. Nevertheless, we expect these changes to be small in our combined analysis of net-kaon fluctuations and $\bar{B}/B$-ratios.

The shown errors in our results base entirely on the errors reported for the analyzed data. Additional uncertainties, stemming from limitations in our framework, have not been included. Different aspects that could lead to a refined analysis are, for example:
(i) If the pion density in the fireball is large and the duration of the late hadronic stage long enough, the regeneration and subsequent decay of K^* resonances provides an additional source of fluctuations in the net-kaon number. The impact of even only a partial isospin randomization [40,41] is to bring a distribution closer to the corresponding Skellam limit as we discussed in [36] in the case of net-proton fluctuations. To describe the data [15] on net-kaon fluctuations in this case would imply an enhancement of the chemical freeze-out conditions. Quantitative predictions of this effect would depend on the made assumptions.
(ii) Exact global charge conservation realized on an event-by-event basis can cause large effects on the fluctuations. This effect was discussed, for example, in [42–45] suggesting a future study in a canonical ensemble formulation.
(iii) Fluctuations in the number of participants for a given centrality class can sizeably influence the measured net-particle number fluctuations [44]. This effect is stronger for higher-order cumulants and smaller beam energies, and is more pronounced for central than very peripheral collisions. Its inclusion into the theoretical framework could potentially affect the results on freeze-out conditions deduced from fluctuation observables in a refined analysis.

Our work provides a baseline which neglects dynamical as well as critical fluctuation effects on the net-kaon number fluctuations. First estimates for the impact of critical fluctuations on these will be reported elsewhere.

Acknowledgements The work of M. Bluhm is funded by the European Union's Horizon 2020 research and innovation program under the Marie Skłodowska Curie grant agreement No 665778 via the National Science Center, Poland, under grant Polonez UMO-2016/21/P/ST2/04035. M. Nahrgang acknowledges the support of the program "Etoiles montantes en Pays de la Loire 2017". This research was supported in part by the ExtreMe Matter Institute (EMMI) at the GSI Helmholtzzentrum für Schwerionenforschung, Darmstadt, Germany. The authors acknowledge fruitful discussions within the framework of the BEST Topical Collaboration. The authors thank P. Alba, R. Bellwied, V. Mantovani Sarti and C. Ratti for discussions at the early stages of this work and X. Luo for providing the data in [15].

Data Availability Statement This manuscript has no associated data or the data will not be deposited. [Authors' comment: The experimental data shown in this work can be found in the corresponding publications or obtained by contacting the experimental collaborations directly.]

Funded by SCOAP[3].

References

1. R. Bellwied, J. Noronha-Hostler, P. Parotto, I. Portillo Vazquez, C. Ratti, J. M. Stafford, arXiv:1805.00088 [hep-ph] (2018)
2. Y. Aoki, G. Endrodi, Z. Fodor, S.D. Katz, K.K. Szabo, Nature **443**, 675 (2006). arXiv:hep-lat/0611014
3. S. Borsanyi et al. [Wuppertal-Budapest Collaboration]. JHEP **1009**, 073 (2010). arXiv:1005.3508 [hep-lat]

4. A. Bazavov et al. Phys. Rev. D **85**, 054503 (2012). arXiv:1111.1710 [hep-lat]
5. J. Berges, K. Rajagopal, Nucl. Phys. B **538**, 215 (1999). arXiv:hep-ph/9804233
6. A.M. Halasz, A.D. Jackson, R.E. Shrock, M.A. Stephanov, J.J.M. Verbaarschot, Phys. Rev. D **58**, 096007 (1998). arXiv:hep-ph/9804290
7. J. Cleymans, H. Oeschler, K. Redlich, S. Wheaton, Phys. Rev. C **73**, 034905 (2006). arXiv:hep-ph/0511094
8. F. Becattini, J. Manninen, M. Gazdzicki, Phys. Rev. C **73**, 044905 (2006). arXiv:hep-ph/0511092
9. A. Andronic, P. Braun-Munzinger, J. Stachel, Phys. Lett. B **673**, 142 (2009) (**Erratum: [Phys. Lett. B 678, 516 (2009)**). arXiv:0812.1186 [nucl-th]
10. A. Andronic, P. Braun-Munzinger, K. Redlich, J. Stachel, J. Phys. G **38**, 124081 (2011). arXiv:1106.6321 [nucl-th]
11. M. Kitazawa, M. Asakawa, H. Ono, Phys. Lett. B **728**, 386 (2014). arXiv:1307.2978 [nucl-th]
12. M. Sakaida, M. Asakawa, M. Kitazawa, Phys. Rev. C **90**(6), 064911 (2014). arXiv:1409.6866 [nucl-th]
13. P. Alba, W. Alberico, R. Bellwied, M. Bluhm, V. Mantovani Sarti, M. Nahrgang, C. Ratti, Phys. Lett. B **738**, 305 (2014). arXiv:1403.4903 [hep-ph]
14. S. Borsanyi, Z. Fodor, S.D. Katz, S. Krieg, C. Ratti, K.K. Szabo, Phys. Rev. Lett. **113**, 052301 (2014). arXiv:1403.4576 [hep-lat]
15. L. Adamczyk et al., [STAR Collaboration]. Phys. Lett. B **785**, 551 (2018). arXiv:1709.00773 [nucl-ex]
16. J.N. Guenther, R. Bellwied, S. Borsanyi, Z. Fodor, S.D. Katz, A. Pasztor, C. Ratti, K.K. Szab, Nucl. Phys. A **967**, 720 (2017). arXiv:1607.02493 [hep-lat]
17. J. Adams et al., [STAR Collaboration]. Phys. Rev. Lett. **98**, 062301 (2007). arXiv:nucl-ex/0606014
18. M.M. Aggarwal et al., [STAR Collaboration]. Phys. Rev. C **83**, 024901 (2011). arXiv:1010.0142 [nucl-ex]
19. F. Zhao [STAR Collaboration], PoS CPOD **2013**, 036 (2013)
20. P. Alba, R. Bellwied, M. Bluhm, V. Mantovani Sarti, M. Nahrgang, C. Ratti, Phys. Rev. C **92**(6), 064910 (2015). arXiv:1504.03262 [hep-ph]
21. R. Venugopalan, M. Prakash, Nucl. Phys. A **546**, 718 (1992)
22. F. Karsch, K. Redlich, A. Tawfik, Eur. Phys. J. C **29**, 549 (2003). arXiv:hep-ph/0303108
23. F. Karsch, K. Redlich, A. Tawfik, Phys. Lett. B **571**, 67 (2003). arXiv:hep-ph/0306208
24. A. Tawfik, Phys. Rev. D **71**, 054502 (2005). arXiv:hep-ph/0412336
25. S. Borsanyi, Z. Fodor, S.D. Katz, S. Krieg, C. Ratti, K.K. Szabo, Phys. Rev. Lett. **111**, 062005 (2013). arXiv:1305.5161 [hep-lat]
26. S. Mukherjee, M. Wagner, PoS CPOD **2013**, 039 (2013). arXiv:1307.6255 [nucl-th]
27. S. Borsanyi, Z. Fodor, S.D. Katz, S. Krieg, C. Ratti, K. Szabo, JHEP **1201**, 138 (2012). arXiv:1112.4416 [hep-lat]
28. C. Patrignani et al. [Particle Data Group], Chin. Phys. C **40**(10), 100001 (2016)
29. P. Alba, Phys. Rev. D **96**(3), 034517 (2017). arXiv:1702.01113 [hep-lat]
30. P. Alba, V. Mantovani Sarti, J. Noronha, J. Noronha-Hostler, P. Parotto, I. Portillo Vazquez, C. Ratti, Phys. Rev. C **98**(3), 034909 (2018). arXiv:1711.05207 [nucl-th]
31. S. Chatterjee, D. Mishra, B. Mohanty, S. Samanta, Phys. Rev. C **96**(5), 054907 (2017). arXiv:1708.08152 [nucl-th]
32. F. Karsch, K. Redlich, Phys. Lett. B **695**, 136 (2011). arXiv:1007.2581 [hep-ph]
33. P. Garg, D.K. Mishra, P.K. Netrakanti, B. Mohanty, A.K. Mohanty, B.K. Singh, N. Xu, Phys. Lett. B **726**, 691 (2013). arXiv:1304.7133 [nucl-ex]
34. V.V. Begun, M.I. Gorenstein, M. Hauer, V.P. Konchakovski, O.S. Zozulya, Phys. Rev. C **74**, 044903 (2006). arXiv:nucl-th/0606036
35. J. Fu, Phys. Lett. B **722**, 144 (2013)
36. M. Nahrgang, M. Bluhm, P. Alba, R. Bellwied, C. Ratti, Eur. Phys. J. C **75**(12), 573 (2015). arXiv:1402.1238 [hep-ph]
37. M. Bluhm, M. Nahrgang, S.A. Bass, T. Schäfer, Eur. Phys. J. C **77**(4), 210 (2017). arXiv:1612.03889 [nucl-th]
38. S. Chatterjee, R.M. Godbole, S. Gupta, Phys. Lett. B **727**, 554 (2013). arXiv:1306.2006 [nucl-th]
39. A. Bazavov et al. Phys. Rev. Lett. **109**, 192302 (2012). arXiv:1208.1220 [hep-lat]
40. M. Kitazawa, M. Asakawa, Phys. Rev. C **85**, 021901 (2012). arXiv:1107.2755 [nucl-th]
41. M. Kitazawa, M. Asakawa, Phys. Rev. C **86** (2012) 024904 (**Erratum-ibid. C 86 (2012) 069902**). arXiv:1205.3292 [nucl-th]
42. M. Nahrgang, T. Schuster, M. Mitrovski, R. Stock, M. Bleicher, Eur. Phys. J. C **72**, 2143 (2012). arXiv:0903.2911 [hep-ph]
43. A. Bzdak, V. Koch, V. Skokov, Phys. Rev. C **87**(1), 014901 (2013). arXiv:1203.4529 [hep-ph]
44. P. Braun-Munzinger, A. Rustamov, J. Stachel, Nucl. Phys. A **960**, 114 (2017). arXiv:1612.00702 [nucl-th]
45. A. Rustamov [ALICE Collaboration], Nucl. Phys. A **967**, 453 (2017). arXiv:1704.05329 [nucl-ex]